A novel distributed generation integrated MFUPQC for active-power regulation with enhanced power quality features

Moturu Seshu[1], Kalyana Sundaram[2], Maddukuri Venkata Ramesh[3]
[1]Department of Electrical Engineering, Annamalai University, Chidambaram, India
[2]Department of Electrical and Electronics Engineering, Government Polytechnic College (Deputed from Annamalai University), Nagercoil, India
[3]Department of Electrical and Electronics Engineering, P.V.P Siddhartha Institute of Technology, Vijayawada, India

Article Info

ABSTRACT

The distributed generation (DG) scheme has become significant and advanced energy generation corridor for present power distribution system. This advanced DG scheme offers several merits such as flexible active power transfer, low transmission losses, maximize power efficiency, reduce transmission cost, expanding grid capacity, so on. It is motivated that, integration of such DG system in to multi-parallel feeder distribution system with enhanced power-quality features is considered as major problem statement. The proposed multi-functional unified power-quality conditioner (MFUPQC) device has robust design, reliable performance; specifically for addressing the voltage-current affecting PQ issues, regulation of active-power in multi-parallel distribution system. The fundamental goal of the MFUPQC device has been to operate as both a PQ improvement device and a DG integration device by implementing a new universal fundamental vector reference (UFVR) control algorithm. The suggested innovative control algorithm extracts the fundamental voltage and current reference signals with low computational response delay, simple mathematical formulations and without additional transformations which are also major problems identified in classical control schemes. This work focuses on design, operation and performance of MFUPQC device has been evaluated in both PQ and DG operations in a multi-parallel feeder distribution system through MATLAB/Simulink computing platform. The simulation results are illustrated with possible interpretation and analysis.

Corresponding Author:

Moturu Seshu
Department of Electrical Engineering, Annamalai University
Chidambaram, Tamilnadu, India
Email: moturuseshu.eee@gmail.com

1. INTRODUCTION

A multi-feeder network presented in [1]-[3], it is the best choice for secondary distribution system while regulating the active power-sharing between the multi-parallel feeders by employing advanced distribution generation (DG) scheme [4]. In this realm, it acts as energy back-up for distributing the continuous active power to load with respect to demand during sudden interruptions, grid-islanding operations [5]-[9]. The advanced DG technique is adopted for maximizing the required load demand by using micro renewable energy sources (MRES) [10]. Also, the MRES associated DG scheme offers several merits such as flexible active power transfer, low transmission losses, maximize power efficiency, reduce transmission cost, expanding grid capacity, so on. The DG scheme utilizing the various renewable sources like wind-energy, solar-photovoltaic (PV), biomass, tidal energies, so on. Amid of several MRES, the solar-

PV becomes most suitable and best choice for DG scheme due to virtuous, low running cost, flexible power transfer, no fuel, more operating life and plentiful nature, so on. It is noted that, such solar-PV powered DG scheme is integrated to multi-parallel feeder distribution system by using advanced power-conditioning devices well with in enhanced power-quality standards [11]-[15].

The greater importance of power-quality (PQ) has a great recognition in multi-parallel feeder distribution network due to critical impacts on utility-grid system and end-level customers. It has become widespread as a result of the use of enormous-sized switch-mode converters for energy conversion, arc heating systems, intermittent speed motors, and reconfiguration of large non-linear dynamic loads at the secondary level of distribution, all of which cause PQ deviations and distortions [16], [17]. This PQ problem prompts the system frequency, grid current, and grid terminal voltage since they are non-sinusoidal and have harmonised components. Harmonic current imperfections, reactive power decrease, non-ideal power factor, and imbalanced loads are some of the most common consequences and causes of poor quality of current waveshape. However, the effects and reasons for voltage quality result in harmonic voltage imperfections, voltage variations, voltage sag/swells, and unbalanced voltage, indicating polluted power at the common point (PCC) of the multi-parallel feeding distribution network [18], [19].

In this context, several power engineers must develop current PQ enhancement devices that employ customised power conditioning (CPC) technologies [20]. This CPC approach employs custom-power devices to address both voltage and current relative PQ issues, yielding a multi-parallel feeder which can be sinusoidal in shape, fundamental type, balanced waveform, and linear [21], [22]. Various multi-parallel feeder CPC devices have been classified based on specific PQ effects and difficulties, such as I-PFC [23], I-DVR [24], I-UPQC [25], and so on. Among the aforementioned devices, the MFUPQC device is specifically designed for multi-parallel feeder distribution networks. It can distribute and interchange active-reactive power across feeders while properly compensating for both voltage-current allied PQ concerns and ensuring quality power in a multi-parallel feeder distribution network [26], [27].

The arrangement of the MFUPQC circuit is detailed in [28], and it was greatly enhanced by placing numerous 3-level voltage-source inverters (VSIs) in a sequential configuration. Numerous VSIs are created by connecting multiple parallel feeders as shunt-series and shunt-shunt interconnection over a common DC-link source. During DG mode, the generated power from solar-PV is immediately incorporated into the multi-parallel feeders via an extra power-electronic interface consisting of a DG-VSI and a front-end DC-DC boost converter. Furthermore, the DG operations are regulated utilising additional droop DG control systems, increasing their size, complexity and expenses of the compensation approach, as described in [29]. The fundamental goal of the MFUPQC device is to be the best choice for both PQ operations and DG modes by employing a workable controller [30].

The most common reference voltage-current extraction systems are synchronous reference Id-Iq frame (SRF) control [31], whereas instantaneous PQ real-power (IRP) control schemes are investigated in [32]. These control techniques have several constraints, such as complicated synchronous transformations, complex mathematical formulation, and a long computational reaction delay. Furthermore, typical control techniques generate a high frequency-based reference signals, which raise dv/dt switching stress, high switching loss, and reduces the system efficiency. To address the aforementioned challenges, an innovative and simple universal basic vector reference (UFVR) control method has been suggested, which extracts the basic voltage-current reference control signals and generates a workable switching pattern to the VSIs of the MFUPQC device. The proposed UFVR controlled MFUPQC device has flexible and robust performance; specifically for addressing the compensation of voltage-current affecting PQ issues. And, also regulation of sharing the active-power is done towards the multi-parallel distribution system during DG operation. This work focuses on design and performance of UFVR with MFUPQC device in multi-parallel feeding distribution network under DG and PQ operations has been evaluated by utilizing the MATLAB/Simulink platform. The simulation results are illustrated with possible interpretation and analysis.

2.   PROPOSED METHOD

The block diagram of the proposed GFVR controller fed DG integrated MFUPQC device is shown in Figure 1. The MFUPQC device conducts both PQ enhancement and DG operations using three 3-level VSIs (VSI-A, VSI-B, and VSI-C) coupled in back-to-back arrangement. In this case, VSI-A is incorporated into feeder-1 as a series connection and enables to mitigate all voltage-related PQ concerns in the particular feeder-1. The other VSI-B, VSI-C, is incorporated into feeder-2 as a series-shunt connection and is configured to mitigate any voltage and current-related PQ concerns in the corresponding feeder. These three VSIs are powered by a common DC-link source capacitor ($C_{dc.s}$) that provides a constant DC voltage of ($V_{dc.s}$). During PQ mitigation mode, the three VSIs of the MFUPQC device operate as active-power filters, counteracting the distinct PQ signatures in feeders-1 and 2. The VSI-A, B of the MFUPQC device in feeder-1, 2 are used as series-active filters to compensate for voltage-related PQ issues such as voltage harmonics,

voltage swells, voltage interruptions, and voltage sag that occur at utility grid source terminal-1, 2. These two VSIs, A and B, are connected to feeders 1 and 2 via 1:1 line interfaced transformers with line filters to eliminate uneven notches. The operation of MFUPQC's VSI-A, B is demonstrated as an active device for mitigating voltage difficulties in accordance with the opposition voltage injection theory. It handles the vital sensitivity load voltage in a well-balanced, low harmonic level sinusoidal-shaped, fundamental manner, with no disruptions and a linear character.
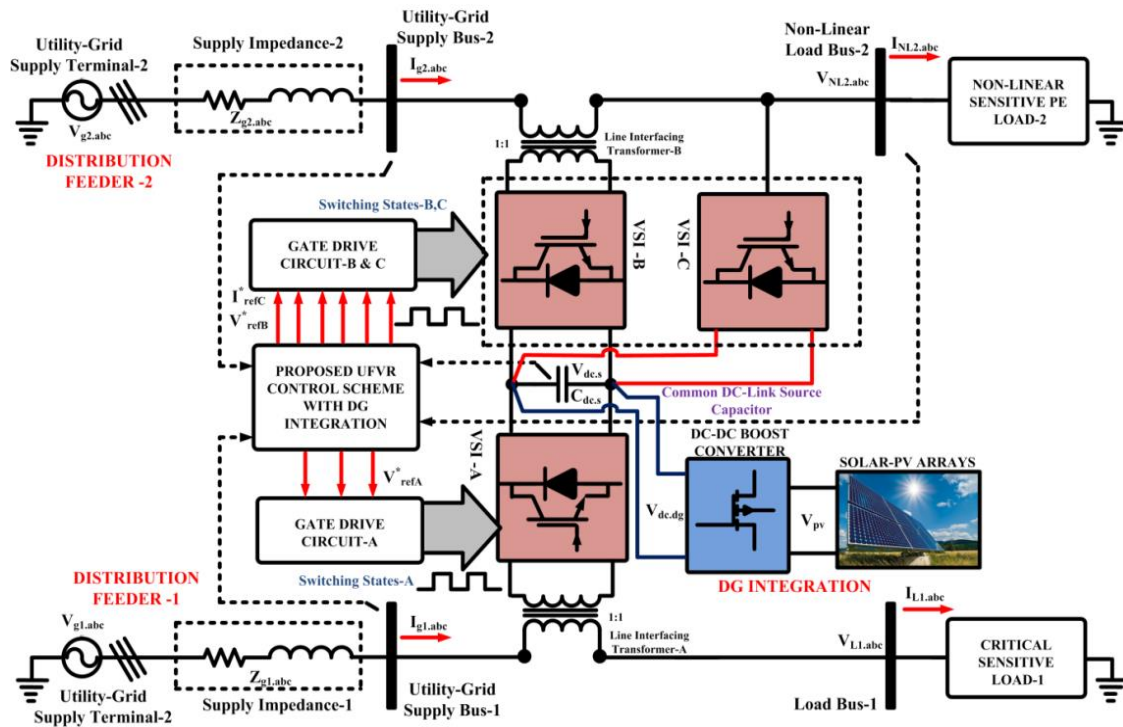
Figure 1. Block diagram of proposed GFVR controller fed DG integrated MFUPQC device

Similarly, the VSI-C of the MFUPQC device in feeder-2 serves as a shunt-active filter to compensate for current-related PQ difficulties caused by non-linear sensitive power-electronic loads. It reduces harmonic current distortions in grid current, balances grid currents, exchanges reactive power, and regulates power factor in utility grid source terminal 2. The VSI-C of MFUPQC functions as an active compensating device for resolving harmonic current difficulties in accordance with the opposition current injection concept. It manages the grid current as sinusoidal shape, harmonic free, balanced and maintain the linear profile through converter side line-filters for elimination of uneven notches in injection current. As a result, the MFUPQC device significantly enhancing the various power-quality issues in PCC of multi-parallel feeders of distribution system while complying with IEEE standards via proposed UFVR control scheme.

In this system, the solar-PV powered DG decreases utility-grid side active power use while solar-PV electricity is available. The solar-PV power was managed utilising a front-end DC-DC boost converter using the incremental-conductance (INC) maximum-power point tracker (MPPT) method. In this regard, solar-PV power has been employed to energise the non-linear PE load and supplies the needed power in response to specific load demand. The working of DG scheme is manifested based on current sharing principle between the solar-PV and utility-grid terminal-2. The required current has been delivered to non-linear PE load based on availability of solar-PV current with continuous power flow during constant irradiance level. If irradiance level is high, the solar-PV delivers the maximum current and utility-grid delivers the minimum current with respect to required load demand. If irradiance level is low, the solar-PV delivers the minimum current and the remaining current has been delivered by utility-grid with respect to required load demand. The major advantages of DG scheme include, it doesn't require additional VSI's and DG controllers, the VSI-C of MFUPQC act as DG inverter and UFVR act as DG controller which offers low-cost, size and compact energy-generation scheme.

3.   PROPOSED UFVR CONTROL ALGORITHM

The suggested UFVR control technique converts the important fundamental reference voltage and current signals to MFUPQC device with no need of sophisticated synchronous conversions or mathematical formulations. Furthermore, reference signals with short response latency aid in the generation of a workable switching pattern to the VSIs of an MFUPQC device during both DG and PQ operations. Furthermore, the proposed control technique generates low/fundamental switching frequency type reference signals, which reducing the dv/dt switching stress and losses while increasing system efficiency. Figure 2 illustrates the suggested UFVR control method. In general, it generates basic reference signals by measuring utility-grid voltages/currents, as well as sensitive critical load currents in feeders 1 and 2. The obtained current and voltage signals are processed to attain vector signals in a synchronous notation with a predefined synchronization angle of (θ_s) via phase-locked loop (PLL). The extracted three-phase utility-grid voltages in both feeders-1, 2 are represented as,

$$
\begin{aligned}
V_{L1.a} &= V_{g1.a} \sin(\theta_s) \\
V_{L1.b} &= V_{g1.b} \sin\left(\theta_s - \frac{2\pi}{3}\right) \\
V_{L1.c} &= V_{g1.c} \sin\left(\theta_s + \frac{2\pi}{3}\right)
\end{aligned}
\tag{1}
$$

$$
\begin{aligned}
V_{NL2.a} &= V_{g2.a} \sin(\theta_s) \\
V_{NL2.b} &= V_{g2.b} \sin\left(\theta_s - \frac{2\pi}{3}\right) \\
V_{NL2.c} &= V_{g2.c} \sin\left(\theta_s + \frac{2\pi}{3}\right)
\end{aligned}
\tag{2}
$$

the non-complex load voltage vectors are represented in (3) as,

$$
V_{sg12.abc} = \left\{ \frac{2}{3} \left(V_{NL12.a}^2 + V_{NL12.b}^2 + V_{NL12.c}^2 \right) \right\}^{1/2}
\tag{3}
$$

for extracting the unit-vector signals as in-phase quadrature form is represented as,

$$
U_{sg12.a} = \frac{V_{L1.a}}{V_{sg12.abc}} = \sin\theta_s
$$

$$
U_{sg12.b} = \frac{V_{L1.b}}{V_{sg12.abc}} = \sin\left(\theta_s - \frac{2\pi}{3}\right)
$$

$$
U_{sg12.c} = \frac{V_{L1.c}}{V_{sg12.abc}} = \sin\left(\theta_s + \frac{2\pi}{3}\right)
\tag{4}
$$

the in-phase quadrature non-complex vector signal $(U_{sg12.abc})$ is approximated with reference voltage magnitude $(V_{ref.m})$ for getting fundamental reference voltage $(V_{ref12.abc}^*)$ signal to both series connected VSI-A, B of MFUPQC device and represented as,

$$
V_{ref12.a}^* = U_{sg12.a} * V_{ref.m}
$$

$$
V_{ref12.b}^* = U_{sg12.b} * V_{ref.m}
$$

$$
V_{ref12.c}^* = U_{sg12.c} * V_{ref.m}
\tag{5}
$$

Likewise, the fundamental reference current signal is generated using the in-phase fractional non-complex vectors signal $(U_{sg12.abc})$ and the magnitude of reference current $(I_{ref.m})$. Using the DC-link control module, the magnitude of the reference current is calculated from the DG solar-PV-current and common DC. It minimizes the flow of currents generated by DC in a common DC capacitor while keeping the voltage constant at the reference value. The current error $(V_{dc.err})$ is determined via a comparison of the reference $(V_{dc.r}^*)$ and real $(V_{dc.s})$ DC capacitor voltages. This is avoided by employing the proportional-integral (PI) controller with careful selection of proportional $(K_{p.dc})$ and integral $(K_{i.dc})$ gain levels. The correct current amplitude $(I_{m.dc})$ is expressed as,

$$
V_{dc.err} = V_{dc.r}^* - V_{dc.s}
\tag{6}
$$

$$I_{m.dc} = K_{p.dc}(V_{dc.err}) + K_{i.dc} \int (V_{dc.err}) dt \tag{7}$$

the extracted solar-PV current in DG mode is represented as (8).

$$I_{m.dg} = I_{L.pv} - I_o \left[exp \left(\frac{V_{pv.dg} + I_{pv.dg}*R_{se}}{\eta V_T} \right) - 1 \right] - \left[\frac{V_{pv.dg} + I_{pv.dg}*R_{se}}{R_{sh}} \right] \tag{8}$$

The in-phase quadrature vector signal ($U_{sg12.abc}$) is approximated with reference current magnitude ($I_{m.dc}$) and extracted solar-PV current ($I_{m.dg}$) for getting fundamental reference current ($I^*_{ref2.abc}$) signal to shunt connected VSI-C of MFUPQC device and represented as (9).

$$I^*_{ref2.a} = U_{sg12.a} * \left(I_{m.dc} + I_{m.dg} \right)$$

$$I^*_{ref2.b} = U_{sg12.b} * \left(I_{m.dc} + I_{m.dg} \right)$$

$$I^*_{ref2.c} = U_{sg12.c} * \left(I_{m.dc} + I_{m.dg} \right) \tag{9}$$

Ultimately, the UFVR control technique produces basic reference signals that help in the development of appropriate switching conditions for the MFUPQC device's VSIs. The MFUPQC device generates switching states to VSI-A and B by distinguishing between the reference voltage signal ($V^*_{ref12.abc}$) and triangular carrier signals ($V_{Cr.abc}$). Based on these switching patterns, VSI-A and B employ a sinusoidal pulse-width modulation (SPWM) circuit to alleviate voltage issues in feeders 1 and 2. Similarly, the current reference signal ($I^*_{ref2.abc}$) is differentiated from the actual current signal ($I_{g1.abc}$) to create switching signals for the MFUPQC's VSI-C. Based on the above switching sequence, the VSI-C handles current issues in Feeder-2 by using a hysteresis current controller (HCC). Figure 3 depicts an overview of the proposed UFVR-controlled MFUPQC device for PQ improvement and DG integration mode.
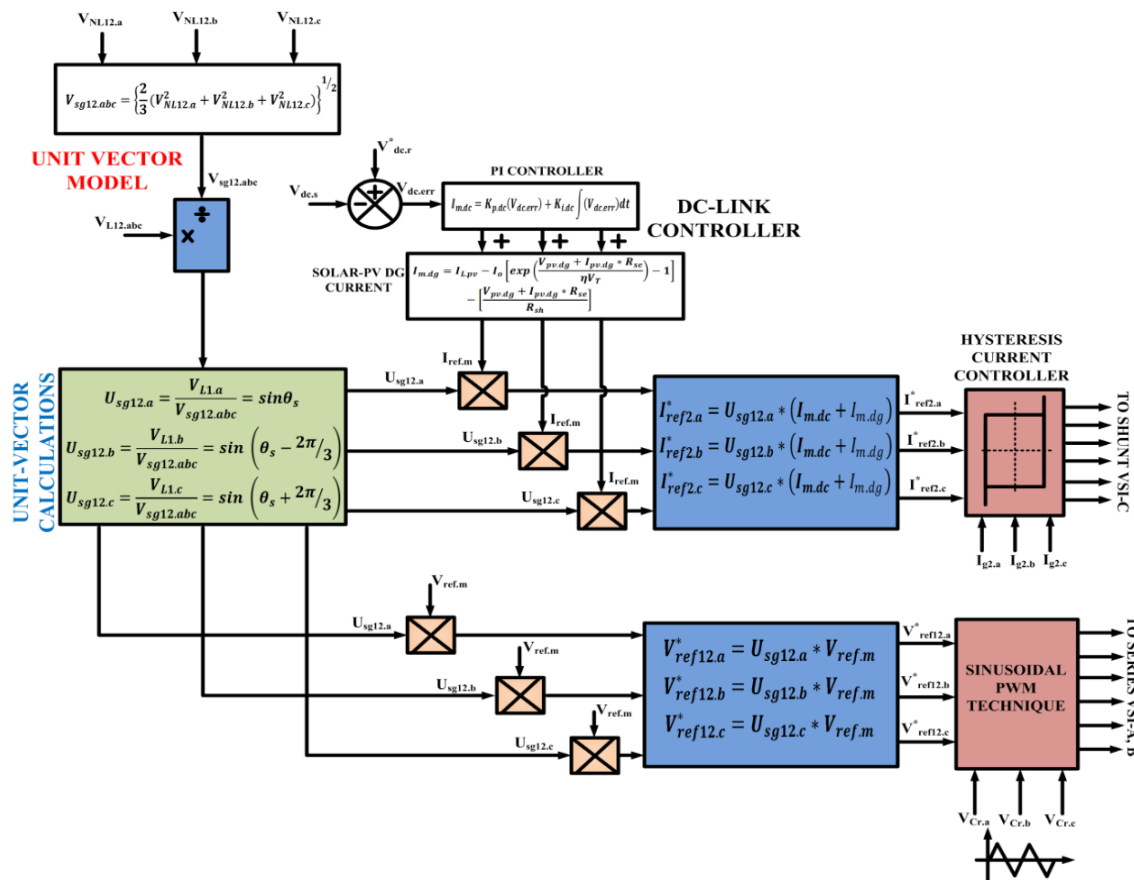

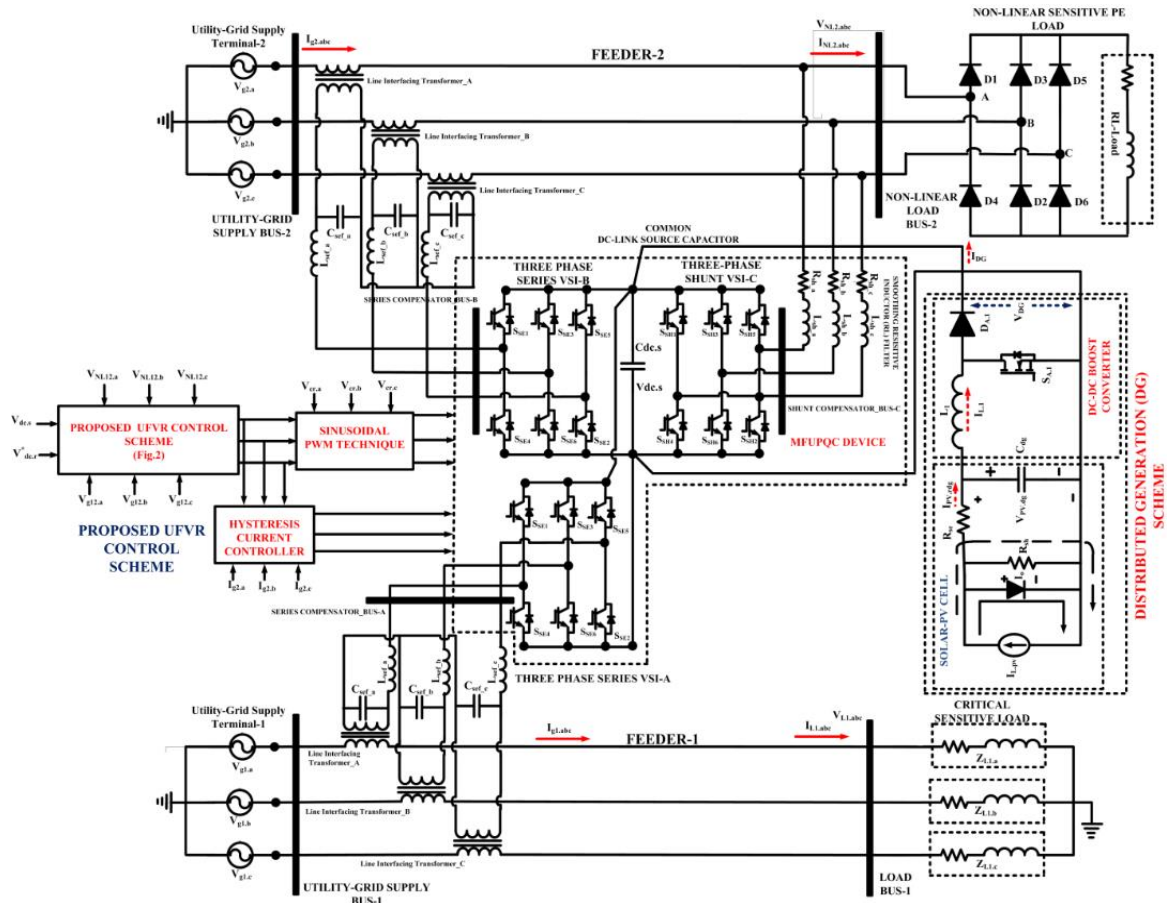Figure 2. Representation of proposed UFVR control scheme

Figure 3. Overall schematic representation of proposed UFVR controlled MFUPQC device for PQ enhancement and DG integration scheme

4. RESULTS AND DISCUSSION

In this paper, the design and performance of a UFVR with an MFUPQC device in a multi-parallel feeder distribution system are assessed under both PQ and DG operations using the MATLAB/Simulink computational platform. Table 1 shows the MATLAB/Simulink data and values. The suggested UFVR with MFUPQC device is tested in a multi-parallel feeder distribution system using voltage-quality improvement, current quality enhancement, and DG integration modes.

Table 1. Simulink data

S. No	Simulink data	Values	
		Feeder-2	Feeder-1
1	Utility-grid supply terminal voltage	$V_{g12.abc}$=415 V_{rms}, 50 Hz	
2	Load parameters	$V_{L2.abc}$=415 Vrms, 50 Hz,	$V_{NL1.abc}$=415 Vrms
		$R_{L1.abc}$=30 Ω, $L_{L1.abc}$=20 mH	$P_{NL1.abc}$=10 KW, $Q_{NL1.abc}$=5 Kvar
3	Supply feeder impedance	$R_{g1.abc}$=0.15 Ω, $L_{g1.abc}$=0.9 mH	
4	1:1 linear line interface transformer	$V_{t.A,B}$=415 V, $P_{t.A,B}$=5 KVA, $X_{t.A,B}$=10% of leakage reactance	
5	Series VSI-A, B line filter	$L_{se.A,B}$ = 3 mH, $C_{se.A,B}$ =100 µF	
6	Shunt VSI-C line filter	$R_{sh.C}$= 0.001 Ω, $L_{sh.C}$=10 mH	
7	Common DC-link source capacitor	$C_{dc.s}$ =1,500 µF, $V_{dc.s}$=880 V	
8	Solar-PV DG specifications	$P_{pv.dg}$=440 V, $I_{pv.dg}$= 20 A, P_{dg}=10 KW	
9	PI controller	$K_{p.dc}$=1.5, $K_{i.dc}$=0.1	

4.1. Performance evaluation of proposed UFVR controlled MFUPQC device for voltage-quality enhancement in feeder-1

Figure 4 in Appendix depicts the simulation results of the recommended UFVR-controlled MFUPQC device for voltage PQ concerns on feeder 1. Figure 4(a) shows that the feeder-1 is powered by a three-phase individual utility grid with a fundamental supply frequency of F_{g1}-50 Hz and a supply voltage of

$V_{g1.abc}$-415 Vrms. Feeder-1 has a three-phase critical sensitive linear load that protects against different voltage-related PQ concerns that may arise in the utility-grid supply voltages. Voltage harmonics, voltage swell, voltage interruptions, and voltage sags constantly impede the very sensitive load voltage in feeder-1. Utility-grid voltage is basic, sinusoidal, and steady throughout pre-existing voltage problems before t-0.15 sec. As seen in Figure 4(a), the utility-grid voltage was distorted at the time instant 0.15 sec<t<0.25 sec as a result of the presence of voltage harmonics, raising the critical sensitive load voltage. In this regard, the in-phase opposition voltage injection concept has allowed the suggested UFVR-controlled series VSI-A of the MFUPQC device to compensate for voltage harmonics while preserving the fundamental nature and sinusoidal form of the sensitive load voltage, as shown in Figure 4(b). At 340 V, the utility-grid voltage stays sinusoidal and stable during the pre-happened voltage surge that occurred before t-0.35sec. Voltage-swell caused the utility-grid voltage to rise dramatically to 510 V at the time instant 0.35 sec<t<0.45 sec, which had an impact on the important sensitive load voltage's ability to function continuously, as shown in Figure 4(a).

Accordingly, by extracting an additional voltage of 170 V and keeping the critical dependent load voltage unchanged and balanced at 340 V, the proposed UFVR regulated series VSI-A of the MFUPQC system is allowed to adjust the amount of voltage swells through in-phase opposition principle, as shown in Figure 4(b). Utility-grid voltage is sinusoidal and stable at 340 V for pre-occurred power disturbances prior to t-0.55sec. Unexpected voltage interruptions caused the utility-grid voltage to drop to 0 V at the time instant 0.55sec<t<0.65sec, which had an impact on the constant, steady operation of the critical, sensitive load voltage, as shown in Figure 4(a). In this sense, by injecting the necessary voltage of 340 V and keeping the critical sensitive load voltage constant and balanced with a value of 340 V, the proposed UFVR regulated series VSI-A of the MFUPQC equipment is successfully allowed to compensate because of voltage distractions via the in-phase opposing principle, as shown in Figure 4(b).

Utility-grid voltage stays sinusoidal and stable at 340 V throughout pre-occurred voltage sags prior to t-0.75 sec. Voltage sags caused the utility-grid voltage to decrease dramatically with a value of 170 V at the time instant 0.75 sec<t<0.85 sec, which had an impact on the continuous, steady functioning of the critical sensitive load voltage as shown in Figure 4(a). Accordingly, by injecting the necessary voltage of 170 V and keeping the critical sensitive load voltage constant and balanced at 340 V, the suggested UFVR regulated series VSI-A of the MFUPQC equipment is allowed to adjust the amount of voltage drops through in-phase opposing principle, as shown in Figure 4(b). Figure 4(c) illustrates how the suggested UFVR control algorithm isolates the essential reference voltage signal that aids in injecting the necessary compensating voltage for enhancing the voltage quality concerns. According to IEEE-519/2022 standards, Figures 4(d) and 4(e) shows the THD spectrum of utility-grid voltage during voltage harmonic distortions in feeder-1, where a value of 20.62% is measured, and during compensating during voltage harmonics in essential responsive load voltage, a value of 0.82% is measured.

4.2. Performance evaluation of proposed UFVR controlled MFUPQC device for voltage-quality enhancement in feeder-2

The simulation results of the suggested UFVR-regulated MFUPQC apparatus for feeder 2's voltage PQ problems are shown in Figure 5 in Appendix. As seen in Figure 5(a), the feeder-2 is operated by a 3-phase individual utility grid with a basic supply frequency of Fg2-50 Hz and a supply voltage of Vg2.abc-415 Vrms. In feeder-2, a three-phase non-linear PE load was connected as a DBR load. This load is shielded from various voltage-related PQ issues that may arise in the utility-grid supply voltage. Non-linear DBR load voltage in feeder-2 is continuously hindered by voltage issues such as voltage harmonics, voltage swell, and voltage sags. Utility-grid voltage is basic frequency, sinusoidal, and steady throughout pre-existing voltage problems before t-0.25 sec. The existence of 5th and 7th-degree harmonics in the voltage caused the utility-grid voltage to be damaged between 0.25 and 0.35 seconds, leading in a non-linear DBR load voltage, as seen in Figure 5(a). In this sense, the proposed UFVR-controlled series VSI-B of the MFUPQC device has been made possible to rectify voltage harmonics through the use of the in-phase opposition voltage injection idea, while maintaining the fundamental characteristics and sinusoidal shape of the non-linear DBR load voltage, as shown in Figure 5(b). At 340 V, the utility-grid voltage stays sinusoidal and stable during the pre-happened voltage surge that occurred prior to t-0.45 sec. Voltage-swell caused the utility-grid voltage to rise marginally to 510 V at the time instant 0.45 sec<t<0.55 sec, which has an effect on the non-linear DBR load voltage's continuous operation, as shown in Figure 5(a). To compensate for voltage swells using the in-phase opposing principle, the recommended UFVR-controlled series VSI-B of the MFUPQC equipment has been allowed. This has been achieved by extracting an extra voltage of 170 V and keeping the DBR load voltage constant and balanced at 340 V, as shown in Figure 5(b).

Utility-grid voltage stays sinusoidal and stable at 340 V throughout pre-affected voltage sags prior to t-0.65 sec. The utility-grid voltage is notably reduced with an amount of 170 V at the time interval 0.65 sec<t<0.75 sec as a result of voltage sags that hinder the constant, steady operation of the non-linear DBR

voltage, as shown in Figure 5(a). Accordingly, by injecting the necessary voltage of 170 V and keeping the non-linear DBR voltage unchanged as well as balanced at 340 V, the recommended UFVR regulated series VSI-B based MFUPQC equipment is allowed to adjust the amount of voltage sags by means of in-phase opposing principle, as shown in Figure 5(b). As seen in Figure 5(c), the recommended UFVR control approach separates the essential reference voltage signal, which aids in injecting the required compensating voltage to improve voltage quality problems. According to IEEE-519/2022 specifications, as shown in Figures 5(d) and 5(e), the THD spectrum for utility-grid voltage throughout voltage harmonic distortion in feeder-2 is obtained with an accuracy of 20.58%, as well as during compensation of the voltage harmonics in non-linear DBR load voltage is calculated with a value of 1.05%.

4.3. Performance evaluation of proposed UFVR controlled MFUPQC device for current-quality enhancement in feeder-2

The simulation findings of the suggested UFVR-regulated MFUPQC device, which is intended to offset the current PQ issues in feeder 2, are shown in Figure 6 in Appendix. As seen in Figure 6(a), the feeder-2 is powered by a three-phase individual utility grid with a fundamental supply frequency of Fg2-50 Hz and a supply voltage of Vg2.abc-415 Vrms. A three-phase nonlinear DBR is used as the load device in this feeder-2 to convert energy for a range of uses. The massive non-linear DBR load modifies the basic character and sinusoidal shape of the utility-grid/PCC current. The injection of currents that are harmonic through these non-linear DBR loads raises temperature losses and affects the thermal capacities of the remaining loads within the PCC of the distribution network. Thus, the MFUPQC device's proposed UFVR driven VSI-C serves as a shunt-integrated APF. It tackles every PQ issue that currently exists, such as reactive power regulation, load balancing, current harmonic distortions, and increasing feeder-2 utility-grid side power factor. To improve current-relative PQ problems in compliance with IEEE/IEC norms, the UFVR controller primarily enables the acquisition of the fundamental reference current, which helps provide suitable switching conditions to shunt VSI-C of the MFUPQC device.

As seen in Figures 6(b) and 6(c), it controls the utility-grid/PCC current in a sinusoidal manner, balancing it with a non-harmonic fundamental frequency of 21 A. This results in a non-linear DBR load current of 20 A. As seen in Figure 6(d), the MFUPQC device's shunt VSI-C was recently made capable of compensating for harmonic variations in utility-grid current by injecting a 10 A compensating current as an in-phase opposing current injection concept. As seen in Figure 6(e), the utility-grid system has a power factor of unity at the PCC because the utility-grid current is in phase with the PCC voltage. In the UFVR method, the dc-link source capacitor is similarly maintained at 880 V using a shared DC-link controller, as seen in Figure 6(f). As indicated in Figures 6(g) and 6(h), the THD spectrum of the non-linear DBR current in feeder-2 is measured at 30.03%, while the THD spectrum of the utility-grid/PCC current in feeder-2 is measured at 2.96% in accordance with IEEE-519/2022 standards.

The THD comparison and graphical visualisation of utility-grid voltage and critical sensitive/non-linear DBR load voltages for both the proposed UFVR driven MFUPQC devices in feeders 1 and 2 and the conventional SRF are presented in Table 2 and Figure 7. For the regular IRP and the recommended UFVR powered MFUPQC device in feeder 1, Table 3 and Figure 8 present THD comparisons and a graphical representation of the utility-grid/PCC current and sensitive non-linear PE load current.

Table 2. THD comparison of utility-grid voltage and critical sensitive/non-linear DBR load voltages of conventional SRF and proposed UFVR controlled MFUPQC device in feeders-1, 2

THD (%)	Utility-grid voltage	Sensitive load voltage	
		Feeder-1	Feeder-2
Conventional SRF controlled MFUPQC device	20.62% 20.58%	4.56%	4.85%
Proposed UFVR controlled MFUPQC device		0.82%	1.05%

Table 3. THD comparisons of utility-grid/PCC current and sensitive non-linear PE load current of conventional IRP and proposed UFVR controlled MFUPQC device in feeder-1

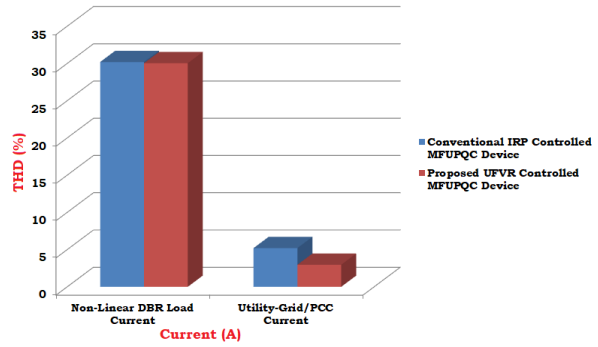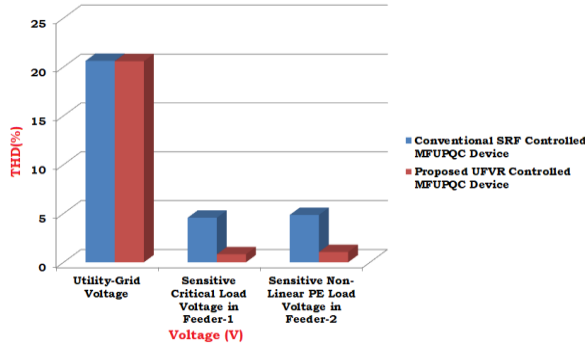| THD (%)	Non-linear DBR load current	Utility grid/PCC current
Conventional IRP controlled MFUPQC device	30.19%	5.20%
Proposed UFVR controlled MFUPQC device	30.03%	2.96%

Figure 7. Graphical view of voltage THD comparison   Figure 8. Graphical view of current THD comparison

4.4. Performance evaluation of proposed UFVR controlled MFUPQC device for solar-PV powered DG integration in feeder-2

Figure 9 in Appendix displays the simulation results of the suggested UFVR driven MFUPQC device for the feeder-2 solar-PV integrated DG system. Feeder-2 usually operated by a three-phase independent utility grid with a basic supply frequency of Fg2-50 Hz and a supply voltage of Vg2.abc-415 Vrms, as shown in Figure 9(a). In this instance, a solar-PV system is used to assess the performance of the UFVR operated MFUPQC device during both PQ improvement and DG integration operations. The VSI-C of the MFUPQC device served as an active power filter at the instant 0 sec<t<1.25 sec, mitigating all current assessed power quality concerns at the utility grid's PCC (when solar irradiance is at 0 W/m^2). The MFUPQC device's VSI-C operated as a DG-VSI during 1.25 sec<t<1.8 sec, providing active power for a non-linear DBR load in accordance with the availability of solar PV power. When solar power is available, this DG technique minimizes the use of utility-grid electricity. The INC-MPPT method regulates the solar power system to extract the greatest amount of power possible.

Assuming that 50% of the solar-PV irradiance level occurs within the time of 1.25 sec<t<1.45 sec, the utility-grid current of 10 A shares the needed non-linear DBR load current of 20 A, with the remaining 10 A being supplied by DG solar-PV operated VSI-C of the MFUPQC apparatus. This current offering concept is illustrated in Figures 9(b) to 9(d). The solar-PV draws an optimal PV voltage of 800 V at 50% of the solar-PV radiation level, as shown in Figure 9(e). This voltage is equivalent to the DC-link voltage, as shown in Figure 9(f). It also draws the highest PV current of approximately 10 A, as shown in Figure 9(g), and the greatest solar power of approximately 6 KW, as shown in Figure 9(h). Similar to this low irradiation level, as shown in Figure 9(i), the DG strategy supplies a minimal active power of 6 KW, while the utility-grid sharing the additional 4 KW of active power in relation to the necessary non-linear DBR load demand power of 10 KW. When the solar-PV radiation level is 100% during the time of 1.45 sec<t<1.8 sec, the utility-grid current of 5A shares the necessary non-linear DBR load current of 20 A, with the remaining 15 A being supplied by the DG solar-PV operated VSI-C of the MFUPQC apparatus. This current offering principle is illustrated in Figures 9(b) to 9(d).

When the solar PV is operating at 100% solar-PV radiation, as Figure 9(e) illustrates, it can extract an ultimate PV voltage of 800 V, which is equivalent to the voltage of the DC-link, as Figure 9(f) shows. It can also extract the highest PV current of approximately 15 A, as Figure 9(g) shows, and the highest PV power of almost 8 KW, as Figure 9(h) shows. Similar to this, at this high irradiation level, the DG scheme produces an optimal active power of 8KW, with the utility grid contributing the additional 2 KW of active power about the necessary non-linear DBR demand for load power of 10 KW, as shown in Figure 9(i). The comparison of active powers of utility-grid, non-linear PE load and VSI-C injected power in DG integration scheme is illustrated in Table 4.

Table 4. Comparison of active powers of utility-grid, non-linear PE load and VSI-C injected power in DG integration scheme

Time instants	Utility-grid power	VSI-C injected DG power	Non-linear PE load power
0 sec<t<1.25 sec	10 KW	0 KW	10 KW
1.25 sec<t<1.45 sec	4 KW	6 KW	10 KW
1.45 sec<t<1.8 sec	2 KW	8 KW	10 KW

5. CONCLUSION

In this work, a novel UFVR controlled MFUPQC device has been proposed to achieve an effective performance for enhancement of power-quality and solar-PV DG integration operations in utility-grid powered multi-parallel feeder distribution system. It mitigates the both voltage and current appraised PQ issues at PCC of both feeders-1, 2 by using in-phase opposition voltage/current injection principle. The proposed UFVR control algorithm extracts fundamental reference signals without using complex synchronous transformations and mathematical formulations. Also, over the conventional IRP/SRF control algorithms the proposed UFVR algorithm reduces the dv/dt stress, switching losses and maximizing the overall efficiency, so on. Moreover, the usage of utility-grid power has been reduced during DG integration mode; the maximum active power to non-linear PE load has been delivered by solar-PV system with respect to certain load demand. The major advantages of DG scheme include, the operation of DG scheme is done through VSI-C of MFUPQC act as DG-VSI and UFVR act as DG controller which offers low-cost, low size and compact energy-generation scheme over the conventional DG schemes. Using the MATLAB/Simulink computer platform, the functioning and effectiveness of the UFVR with the MFUPQC equipment in the multi-parallel feeder distribution system under both PQ and DG operations are assessed. The simulation results are shown, and the system complies with IEEE-519/2022 requirements.
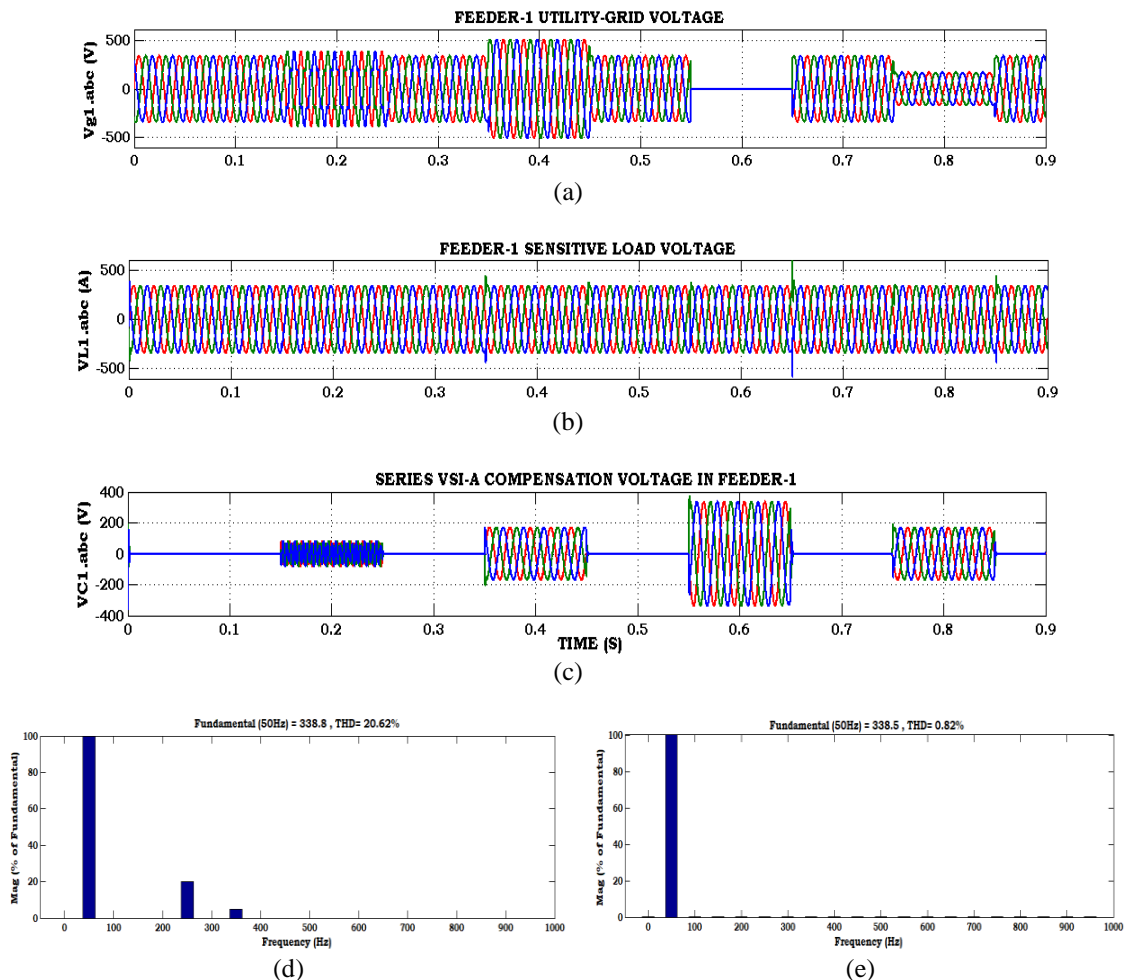
APPENDIX

Figure 4. Simulation results of the UFVR-controlled MFUPQC device for feeder-1 voltage PQ problem compensation; (a) utility-grid voltage, (b) critical sensitive load voltage, (c) series VSI-A compensation voltages in feeder-1, (d) THD spectrum of utility-grid voltage, and (e) THD spectrum of critical sensitive load voltage
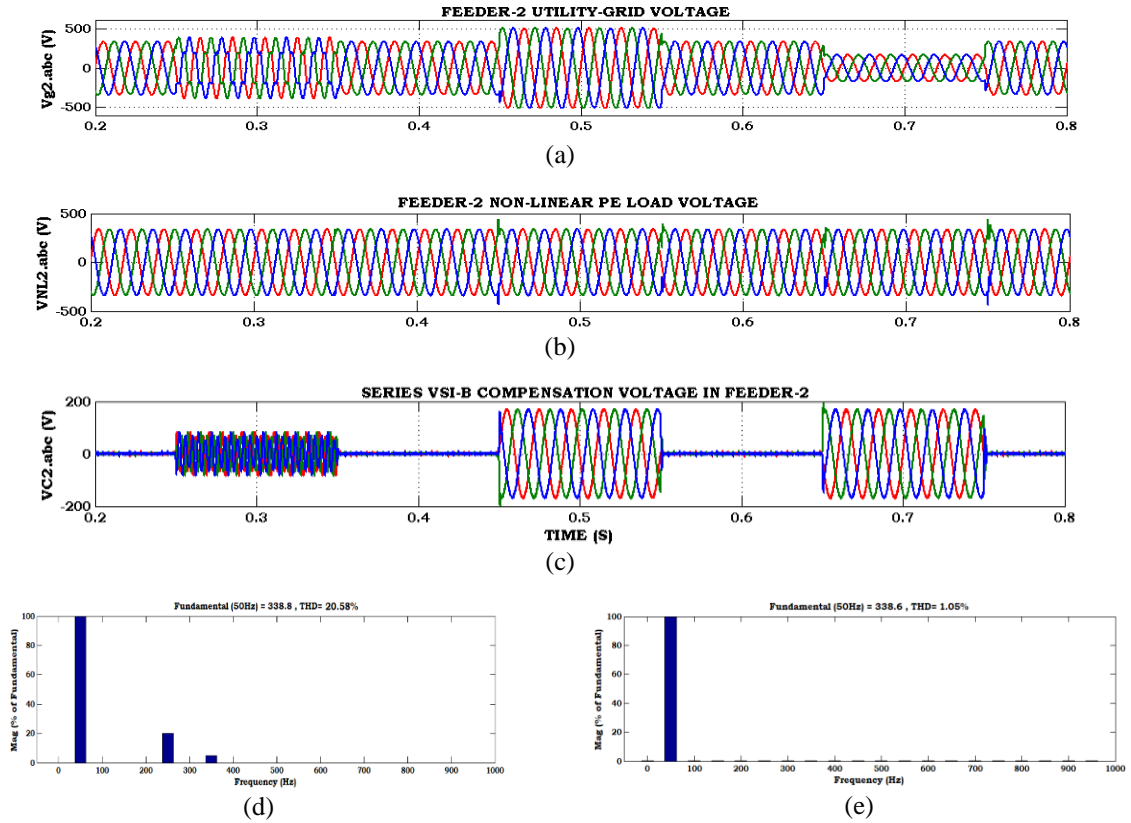
Figure 5. Simulation results of the suggested UFVR-controlled MFUPQC device for feeder-2's voltage PQ problem compensation; (a) utility-grid voltage, (b) non-linear PE load voltage, (c) series VSI-B compensation voltages in feeder-2, (d) THD spectrum of utility-grid voltage, and (e) THD spectrum of non-linear DBR load voltage
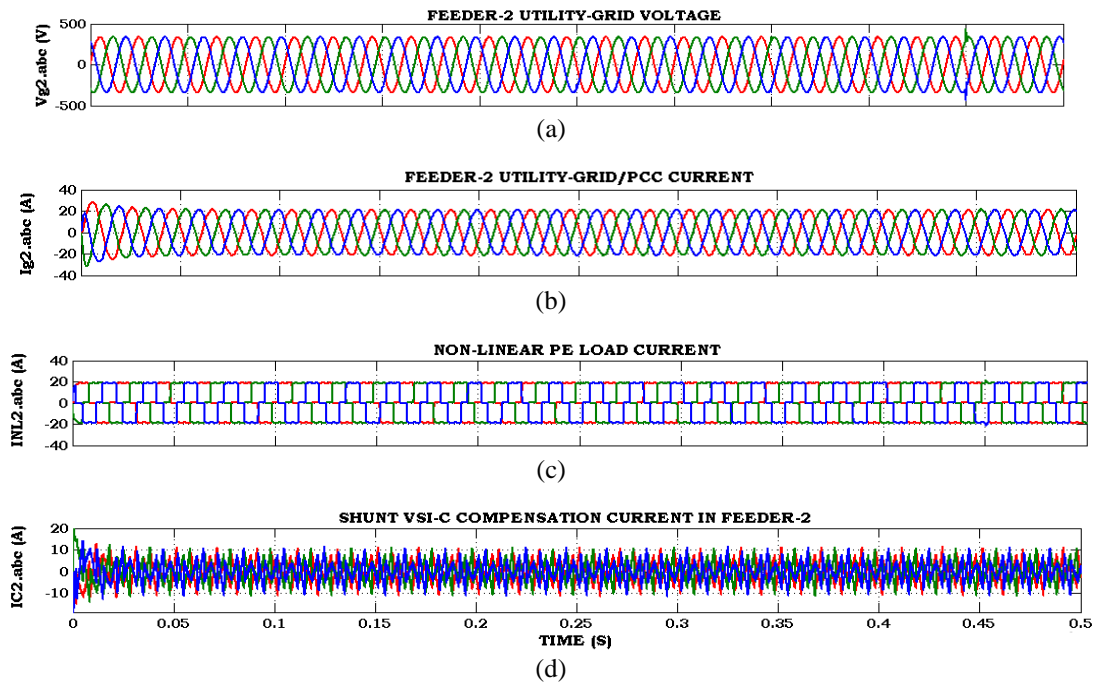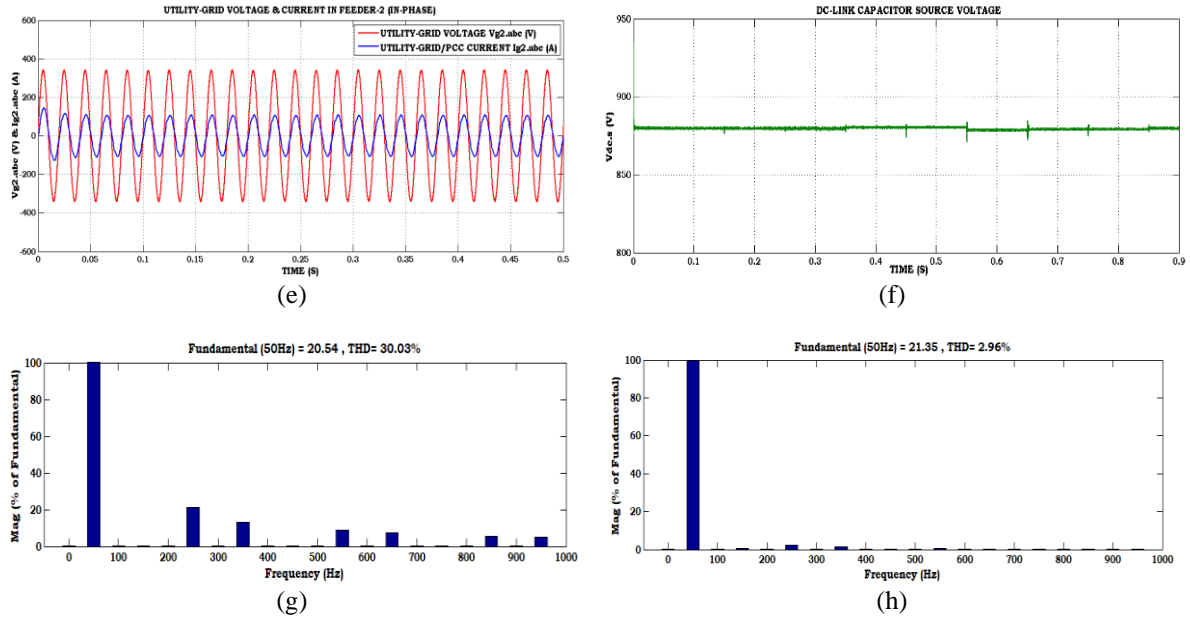

Figure 6. Simulation results of the UFVR-controlled MFUPQC device for feeder-2's current PQ problems compensation; (a) utility-grid voltage, (b) utility-grid current, (c) non-linear PE load current (d) shunt VSI-C compensation currents in feeder-2

(e)

(f)

(g)

(h)

Figure 6. Simulation results of the UFVR-controlled MFUPQC device for feeder-2's current PQ problems compensation; (e) in-phase of utility-grid voltage and current, (f) voltage across DC-link source capacitor, (g) THD spectrum of non-linear DBR load current, and (h) THD spectrum of utility-grid current (*Continued*)
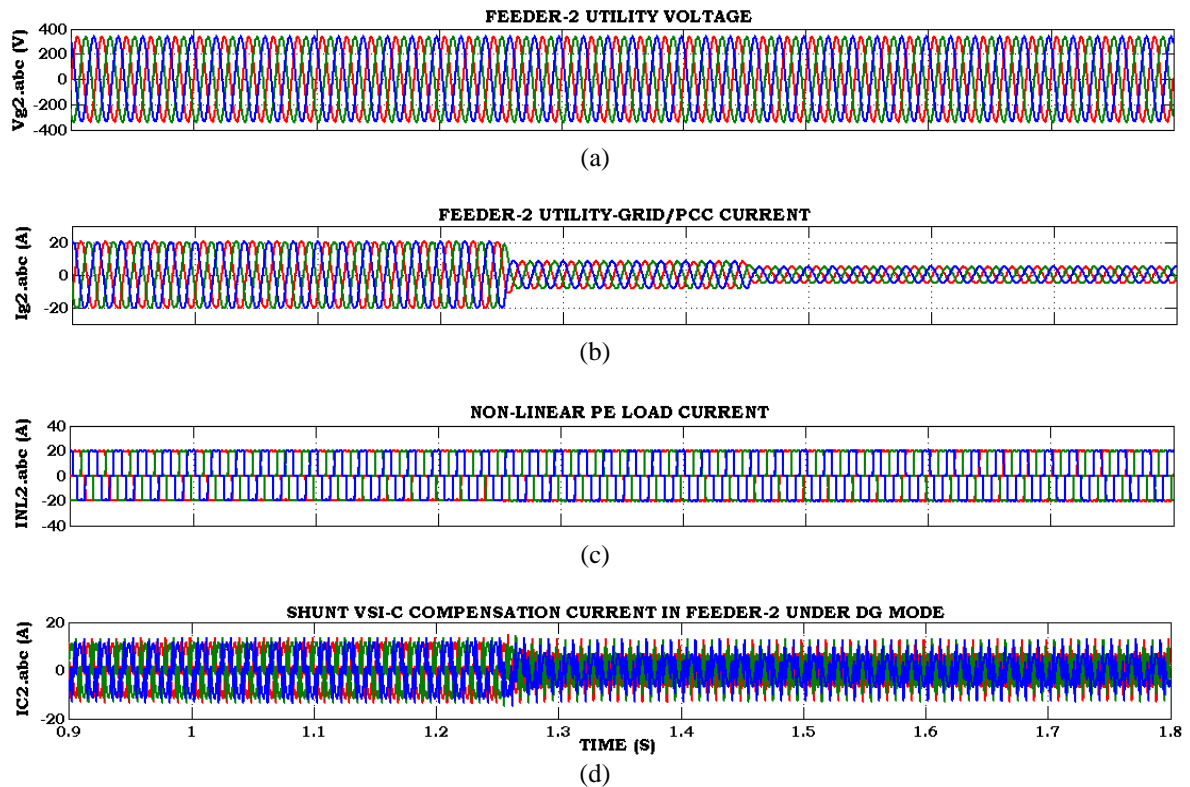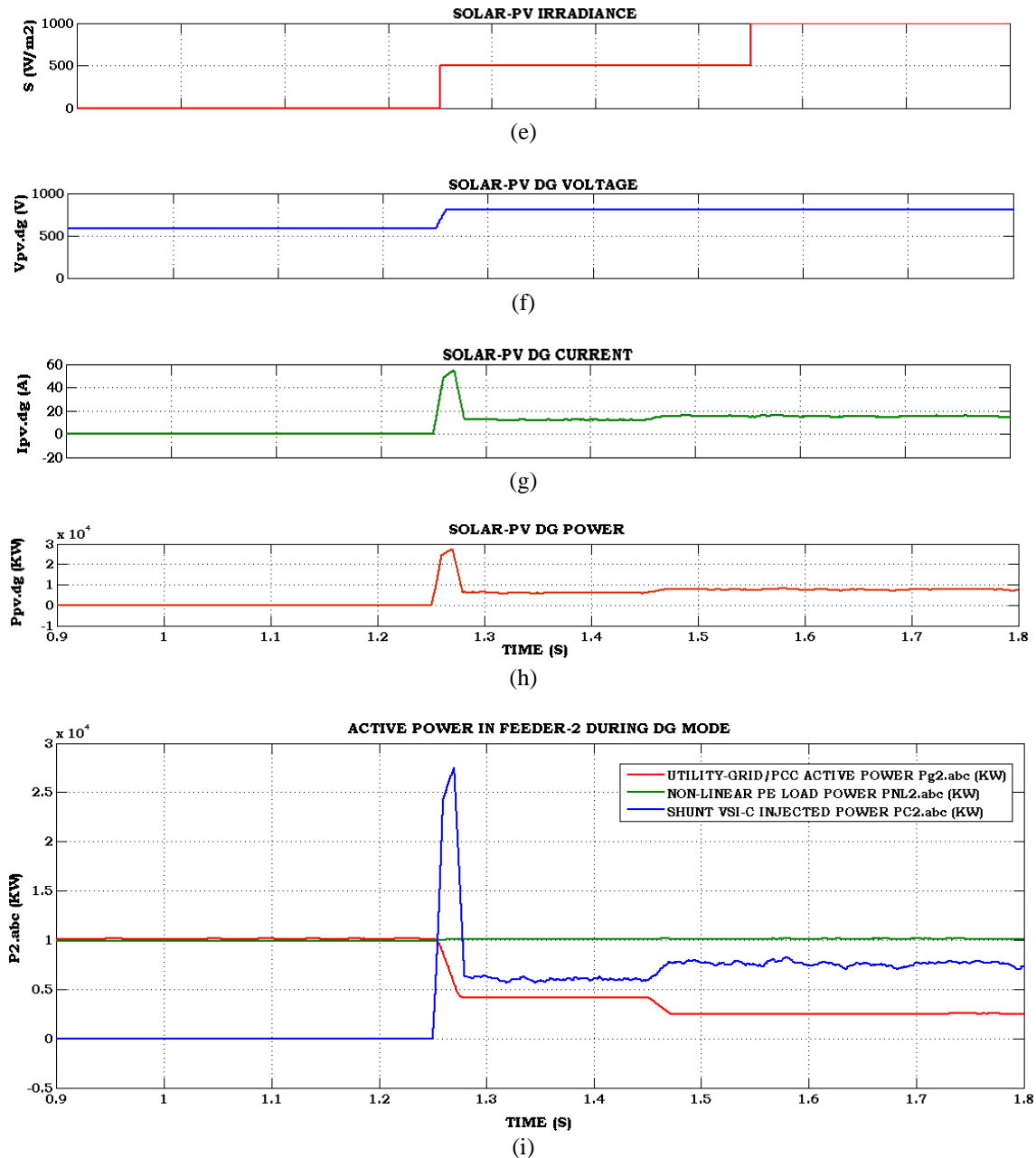

(a)

(b)

(c)

(d)

Figure 9. Simulation results of the UFVR-controlled MFUPQC device for the integration of solar-PV powered DG in feeder-2; (a) utility-grid voltage, (b) utility-grid current, (c) non-linear PE load current, and (d) shunt VSI-C compensation currents in feeder-2

(e)

(f)

(g)

(h)

(i)

Figure 9. Simulation results of the UFVR-controlled MFUPQC device for the integration of solar-PV powered DG in feeder-2; (e) solar-pv irradiance, (f) solar-PV DG voltage, (g) solar-PV DG current, (h) solar-PV power, and (i) active powers of utility-grid, non-linear PE load and VSI-C injected power in DG integration scheme (*Continued*)

REFERENCES

[1] H. Wang, Y. P. Fang, and E. Zio, "Risk assessment of an electrical power system considering the influence of traffic congestion on a hypothetical scenario of electrified transportation system in New York State," *IEEE Transactions on Intelligent Transportation Systems*, vol. 22, no. 1, pp. 142–155, Jan. 2021, doi: 10.1109/TITS.2019.2955359.

[2] F. Bizzarri and A. Brambilla, "Generalized power flow analysis of electrical power systems modeled as mixed single-phase/three-phase sub-systems," *IEEE Transactions on Power Systems*, vol. 35, no. 2, pp. 1284–1293, Mar. 2020, doi: 10.1109/TPWRS.2019.2945137.

[3] A. K. Yadav, P. Tiwari, and R. Maurya, "Power quality conditioning in multifeeder using MC-UPQC," in *International Conference on Electrical and Electronics Engineering, ICE3 2020*, Feb. 2020, pp. 645–649, doi: 10.1109/ICE348803.2020.9122992.

[4] G. Papaefthymiou, M. Houwing, M. P. C. Weijnen, and L. Van Der Sluis, "Distributed generation vs bulk power transmission," in *2008 1st International Conference on Infrastructure Systems and Services: Building Networks for a Brighter Future, INFRA 2008*, 2008, pp. 1–6, doi: 10.1109/INFRA.2008.5439691.

[5]   K. Mahmoud, N. Yorino, and A. Ahmed, "Optimal distributed generation allocation in distribution systems for loss minimization," *IEEE Transactions on Power Systems*, vol. 31, no. 2, pp. 960–969, Mar. 2016, doi: 10.1109/TPWRS.2015.2418333.

[6]   T. Zhao, B. Chen, S. Zhao, J. Wang, and X. Lu, "A flexible operation of distributed generation in distribution networks with dynamic boundaries," *IEEE Transactions on Power Systems*, vol. 35, no. 5, pp. 4127–4130, Sep. 2020, doi: 10.1109/TPWRS.2020.3004765.

[7]   M. Al-Muhaini and G. T. Heydt, "Evaluating future power distribution system reliability including distributed generation," *IEEE Transactions on Power Delivery*, vol. 28, no. 4, pp. 2264–2272, Oct. 2013, doi: 10.1109/TPWRD.2013.2253808.

[8]   P. S. Georgilakis and N. D. Hatziargyriou, "Optimal distributed generation placement in power distribution networks: models, methods, and future research," *IEEE Transactions on Power Systems*, vol. 28, no. 3, pp. 3420–3428, Aug. 2013, doi: 10.1109/TPWRS.2012.2237043.

[9]   J. M. Rondina, N. L. Martins, and M. B. Alves, "Technology alternative for enabling distributed generation," *IEEE Latin America Transactions*, vol. 14, no. 9, pp. 4089–4096, Sep. 2016, doi: 10.1109/TLA.2016.7785938.

[10]   A. H. Alobaidi, S. S. Fazlhashemi, M. Khodayar, J. Wang, and M. E. Khodayar, "Distribution service restoration with renewable energy sources: a review," *IEEE Transactions on Sustainable Energy*, vol. 14, no. 2, pp. 1151–1168, Apr. 2023, doi: 10.1109/TSTE.2022.3199161.

[11]   F. Liu, C. Chen, C. Lin, G. Li, H. Xie, and Z. Bie, "Utilizing aggregated distributed renewable energy sources with control coordination for resilient distribution system restoration," *IEEE Transactions on Sustainable Energy*, vol. 14, no. 2, pp. 1043–1056, Apr. 2023, doi: 10.1109/TSTE.2023.3242357.

[12]   Y. M. Atwa, E. F. El-Saadany, M. M. A. Salama, and R. Seethapathy, "Optimal renewable resources mix for distribution system energy loss minimization," *IEEE Transactions on Power Systems*, vol. 25, no. 1, pp. 360–370, Feb. 2010, doi: 10.1109/TPWRS.2009.2030276.

[13]   A. K. Singh, S. Kumar, and B. Singh, "Solar PV energy generation system interfaced to three phase grid with improved power quality," *IEEE Transactions on Industrial Electronics*, vol. 67, no. 5, pp. 3798–3808, May 2020, doi: 10.1109/TIE.2019.2921278.

[14]   S. J. Steffel, P. R. Caroselli, A. M. Dinkel, J. Q. Liu, R. N. Sackey, and N. R. Vadhar, "Integrating solar generation on the electric distribution grid," *IEEE Transactions on Smart Grid*, vol. 3, no. 2, pp. 878–886, Jun. 2012, doi: 10.1109/TSG.2012.2191985.

[15]   S. Kumar and B. Singh, "A multipurpose PV system integrated to a three-phase distribution system using an LWDF-based approach," *IEEE Transactions on Power Electronics*, vol. 33, no. 1, pp. 739–748, Jan. 2018, doi: 10.1109/TPEL.2017.2665526.

[16]   X. P. Zhang and Z. Yan, "Energy quality: a definition," *IEEE Open Access Journal of Power and Energy*, vol. 7, pp. 430–440, 2020, doi: 10.1109/OAJPE.2020.3029767.

[17]   T. Tarasiuk *et al.*, "Review of power quality issues in maritime microgrids," *IEEE Access*, vol. 9, pp. 81798–81817, 2021, doi: 10.1109/ACCESS.2021.3086000.

[18]   J. Yaghoobi, A. Abdullah, D. Kumar, F. Zare, and H. Soltani, "Power quality issues of distorted and weak distribution networks in mining industry: a review," *IEEE Access*, vol. 7, pp. 162500–162518, 2019, doi: 10.1109/ACCESS.2019.2950911.

[19]   D. Razmi, T. Lu, B. Papari, E. Akbari, G. Fathi, and M. Ghadamyari, "An overview on power quality issues and control strategies for distribution networks with the presence of distributed generation resources," *IEEE Access*, vol. 11, pp. 10308–10325, 2023, doi: 10.1109/ACCESS.2023.3238685.

[20]   E. Hossain, M. R. Tur, S. Padmanaban, S. Ay, and I. Khan, "Analysis and mitigation of power quality issues in distributed generation systems using custom power devices," *IEEE Access*, vol. 6, pp. 16816–16833, 2018, doi: 10.1109/ACCESS.2018.2814981.

[21]   S. Singh and S. S. Letha, "Various custom power devices for power quality improvement: a review," in *2018 International Conference on Power Energy, Environment and Intelligent Control, PEEIC 2018*, Apr. 2018, pp. 689–695, doi: 10.1109/PEEIC.2018.8665470.

[22]   T. S. Saggu and L. Singh, "Comparative analysis of custom power devices for power quality improvement in non-linear loads," in *2015 2nd International Conference on Recent Advances in Engineering and Computational Sciences, RAECS 2015*, Dec. 2016, pp. 1–5, doi: 10.1109/RAECS.2015.7453421.

[23]   G. Satyanarayana, K. N. V. Prasad, G. R. Kumar, and K. L. Ganesh, "Improvement of power quality by using hybrid fuzzy controlled based IPQC at various load conditions," in *2013 International Conference on Energy Efficient Technologies for Sustainability, ICEETS 2013*, Apr. 2013, pp. 1243–1250, doi: 10.1109/ICEETS.2013.6533565.

[24]   M. Shahabadini and H. Iman-Eini, "Improving the Performance of a cascaded h-bridge-based interline dynamic voltage restorer," *IEEE Transactions on Power Delivery*, vol. 31, no. 3, pp. 1160–1167, Jun. 2016, doi: 10.1109/TPWRD.2015.2480967.

[25]   J. Muruganandham, K. Arun, K. Thangaraj, and V. Malarselvam, "Performance analysis of interline unified power flow controller for parallel transmission lines," in *Proceedings of 2015 IEEE International Conference on Electrical, Computer and Communication Technologies, ICECCT 2015*, Mar. 2015, pp. 1–8, doi: 10.1109/ICECCT.2015.7225994.

[26]   V. Khadkikar, "Enhancing electric power quality using UPQC: a comprehensive overview," *IEEE Transactions on Power Electronics*, vol. 27, no. 5, pp. 2284–2297, May 2012, doi: 10.1109/TPEL.2011.2172001.

[27]   Y. M. Esmail, A. H. Kasem Alaboudy, M. S. Hassan, and G. M. Dousoky, "Mitigating power quality disturbances in smart grid using FACTS," *Indonesian Journal of Electrical Engineering and Computer Science*, vol. 22, no. 3, pp. 1223–1235, Jun. 2021, doi: 10.11591/ijeecs.v22.i3.pp1223-1235.

[28]   M. Seshu, P. K. Sundaram, and M. V. Ramesh, "A novel PQ improvement in multi-parallel feeder distribution system using multi-convertible UPQC device," *International Journal of Applied Power Engineering (IJAPE)*, vol. 13, no. 2, p. 382, Jun. 2024, doi: 10.11591/ijape.v13.i2.pp382-395.

[29]   P. V. V. Satyanarayana and P. V. Ramana Rao, "DG integration to distribution system with active power injection control," *International Journal of Power Electronics and Drive Systems*, vol. 11, no. 2, pp. 692–701, Jun. 2020, doi: 10.11591/ijpeds.v11.i2.pp692-701.

[30]   N. S. Rao and P. V. R. Rao, "Novel multi-device unified powerquality conditioner for powerquality improvement," *International Journal of Power Electronics and Drive Systems*, vol. 13, no. 1, pp. 390–400, Mar. 2022, doi: 10.11591/ijpeds.v13.i1.pp390-400.

[31]   M. Kesler and E. Ozdemir, "Synchronous-reference-frame-based control method for UPQC under unbalanced and distorted load conditions," *IEEE Transactions on Industrial Electronics*, vol. 58, no. 9, pp. 3967–3975, Sep. 2011, doi: 10.1109/TIE.2010.2100330.

[32]   K. Palanisamy, J. S. Mishra, I. J. Raglend, and D. P. Kothari, "Instantaneous power theory based unified power quality conditioner (UPQC)," in *2010 Joint International Conference on Power Electronics, Drives and Energy Systems, PEDES 2010 and 2010 Power India*, Dec. 2010, pp. 1–5, doi: 10.1109/PEDES.2010.5712453.

BIOGRAPHIES OF AUTHORS

Moturu Seshu ⓘ 🔳 sc ○ received his M.Tech. degree in Power Systems-High Voltage Engineering from Jawaharlal Nehru Technological University Kakinada, Kakinada, India, in 2011. He is currently working as Assistant Professor in Department of Electrical and Electronics Engineering at P.V.P Siddhartha Institute of Technology, Vijayawada, India. His research work includes renewable energy sources, power quality, and artificial intelligence techniques. He can be contacted at email: moturuseshu.eee@gmail.com.

Kalyana Sundaram ⓘ 🔳 sc ○ received his Ph.D. degree in Power Quality Assessment from Annamalai University, Chidambaram, Tamilnadu, India, in 2017. He is currently Lecturer in Electrical and Electronics Engineering department at Government Polytechnic College Nagercoil, Tamilnadu deputed from Annamalai University. His research interests include power quality, signal processing, artificial neural network, fuzzy logic, and adaptive neuro-fuzzy interface system. He can be contacted at email: kalyansundar7@gmail.com.

Maddukuri Venkata Ramesh ⓘ 🔳 sc ○ received the B.Tech. degree in Electrical and Electronics Engineering from Nagarjuna University in the year 1998 and M.S (Electrical Engineering) from University of Darmstadt Germany in the year 2002. He received Ph.D. degree in the year 2015. From June 2003–March 2010, he worked as an Assistant Professor and since March 2010, he is working as an Associate Professor at P.V.P. Siddhartha Institute of Technology, Vijayawada, India. His research interests include power electronics and drives, power system automation, hybrid vehicle design and renewable energy sources. He published around 50 papers in national and international conferences and international journals. He can be contacted at email: vrmaddukuri@gmail.com.